Comparison of uncertainty quantification methods for mathematical problems in intermediate dimensions

Jacques Peter, Quentin Bennehard

COMPARISON OF UNCERTAINTY QUANTIFICATION METHODS FOR MATHEMATICAL PROBLEMS IN INTERMEDIATE DIMENSIONS

JACQUES PETER, QUENTIN BENNEHARD

ONERA/DAAA, Université Paris-Saclay
BP 80100, FR-91123 Palaiseau Cedex, France
e-mail: jacques.peter@onera.fr quentin.bennehard@onera.fr, www.onera.fr

Key words: Numerical integration, Sparse grids, Generalized Polynomial Chaos, Compressed sensing, Least Angle Regression

Abstract. The efficiency of multidimensional quadrature methods is compared for seven test functions in intermediate dimensions. Following this goal, the numerical evaluations of the mean and variance of the test functions, for two probability density functions, are assessed with respect to (wrt) their known exact values. The retained dimensions (3 to 6) correspond to the number of operational and geometrical uncertain parameters we plan to consider in a near future for realistic sensitivity analysis or robust designs. Most of the numerical quadrature methods rely on a generalized Polynomial Chaos (gPC) defined either by quadrature or by collocation. Two of the gPC collocation techniques, Basis Poursuit Denoise (BPdn) and Least Angle Regression (LAR), search for a sparse gPC while satisfying the collocation equations. Finally, the efficiency of the quadrature methods is discussed in relation with the regularity, the input dimension and the ANOVA decomposition of the test functions.

1 INTRODUCTION

ONERA participated in several cooperative projects devoted to uncertainty quantification (UQ) for computational fluid dynamics (CFD), like the EU projects NODESIM-CFD and UMRIDA or the RTO-AVT-191 group [14, 21, 29, 24]. Uncertainty calculation about complex flows requires significant CPU ressources and does not allow a large comparison of quadrature techniques. Conversely, in this study, we assess the efficiency of a series numerical integration methods, mostly based on generalized Polynomial Chaos (gPC)[32], for the calculation of the mean and variance of seven mathematical test functions. Of course, the retained intermediate dimensions (3 to 6) correspond to the number of uncertain parameters we plan to deal with in a near future in sensitivity analysis or robust designs applications.

2 PDF AND TEST FUNCTIONS

2.1 Classical test functions for numerical integration

Probably, the most widely used test functions for numerical integration are those defined by Genz [10]. This series of five multivariate functions (Oscillatory, product peak, corner peak, Gaussian, C^0, discontinuous) varies the regularity from C^∞ to C^0 and discontinuous and goes

with two families of numerical parameters: the first ones are typically shifts along the axis that do not affect the difficulty of the integration ; on the contrary, the second ones make the functions more stiff/oscillatory. These test functions are very interesting but they do not vary the coupling of the input variables unless incidentally some of the parameters of the second family are zero.
Also interesting are the nine test functions defined by Kocis and Whiten [13] that are all designed to have null mean and unit variance. The first three functions are sums of 1D-functions. The next four functions are product functions with numbers of minima and maxima increasing with 2^n as well as exponentially increasing absolute maximum. The last two functions are sums of two-dimensional components that are themselves products of two one-dimensional functions.
In this study, we consider seven test functions with various regularity and coupling bewteen input variables. In order to quantitatively qualify this coupling, we calculate the number non-zero second-order terms in the ANOVA decomposition divided by the total number of pairs of input variables. Besides, the previous contributions considered integration for the uniform distribution whereas more peaky distributions may be more representative of an uncertain parameter in an engeering problem and may concentrate the integration in zone of discontinuity or, at least, locally low regularity and thus make the integration more difficult. Therefore a constant and also a peaky probability density function (pdf) are considered.

2.2 Probability density functions

We consider both a uniform distribution and a peaky β distribution with two equal exponents.

$$D^U(\boldsymbol{\xi}) = 1/2^n \qquad D^{(2)}(\boldsymbol{\xi}) = \left(\frac{15}{16}\right)^n \prod_{l=1}^{n} (1-\xi_l^2)^2$$

The mean and variance of a function F for these two pdf are denoted as follows:

$$E^u(F) = \int_{[-1,1]^n} F(\boldsymbol{\xi}) D^u(\boldsymbol{\xi}) d\boldsymbol{\xi} \qquad V^u(F) = \int_{[-1,1]^n} (F(\boldsymbol{\xi}) - E^u(F))^2 D^u(\boldsymbol{\xi}) d\boldsymbol{\xi}.$$

$$E^{(2)}(F) = \int_{[-1,1]^n} F(\boldsymbol{\xi}) D^{(2)}(\boldsymbol{\xi}) d\boldsymbol{\xi} \qquad V^{(2)}(F) = \int_{[-1,1]^n} (F(\boldsymbol{\xi}) - E^{(2)}(F))^2 D^{(2)}(\boldsymbol{\xi}) d\boldsymbol{\xi}.$$

2.3 Test functions

The first function is the well-known Ishigami or Homma-Saltelli function [9]. Functions three and four are taken from [13]. The input variable is denoted $\boldsymbol{\xi} \in [-1,1]^n$ and the seven test

functions read:

$$
\begin{aligned}
F_1(\boldsymbol{\xi}) &= \sin(\pi\xi_1) + a\sin^2(\pi\xi_2) + b\ (\pi\xi_3)^4\sin(\pi\xi_1)\\
F_2(\boldsymbol{\xi}) &= \exp(\xi_1 + \frac{\xi_2}{2} + \frac{\xi_3}{3}) + 2\exp(\xi_2 + \frac{\xi_3}{2} + \frac{\xi_4}{3}) + 3\exp(\xi_3 + \frac{\xi_4}{2} + \frac{\xi_5}{3})\\
F_3(\boldsymbol{\xi}) &= \sqrt{\frac{9}{n}}\left(\sum_{j=1}^{n}\sqrt{\xi_j + 1} - \frac{2\sqrt{2}n}{3}\right)\\
F_4(\boldsymbol{\xi}) &= \prod_{j=1}^{n}(-1.2\sqrt{7}\xi_j + \sqrt{7}\xi_j^3)\\
F_5(\boldsymbol{\xi}) &= \gamma_n\prod_{j=1}^{n}\tanh(2\xi_j) + \eta_n\sum_{j=1}^{n}\xi_j \quad \text{with} \quad \gamma_n = \frac{2^{(n-1)/2}}{(2-\tanh(2))^{n/2}} \qquad \eta_n = \sqrt{\frac{3}{2n}}\\
F_6(\boldsymbol{\xi}) &= 0.5/(1+\xi_1^2) + 1/(1+4\xi_2^2)/(1+4\xi_3^2) + 8/(1+16\xi_4^2)/(1+16\xi_5^2)/(1+16\xi_6^2)\\
F_7(\boldsymbol{\xi}) &= |\xi_1|^3 + |\xi_2 + 1/3|^3|\xi_3 - 1/3|^3 + |\xi_4 + 1/2|^3|\xi_5|^3|\xi_6 - 1/2|^3
\end{aligned}
$$

For numerical tests, F_3, F_4 and F_5 are considered in dimension 5.

2.4 Exact mean and variance for uniform distribution

The exact mean and variance of the test functions for the uniform distribution are gathered hereafter. The mean and variance of Ishigami function for D^u are [9]

$$E^u(F_1) = \frac{a}{2} \qquad V^u(F_1) = \frac{a^2}{8} + \frac{b\pi^4}{5} + \frac{b^2\pi^8}{18} + \frac{1}{2}.$$

Considering F_2, we first calculate

$$s(a) = \int_{-1}^{1}\exp(at)D^u(t)dt = \frac{e^a - e^{-a}}{2a}, \qquad \text{then}$$

$$
\begin{aligned}
E^u(F_2) &= 6s(1)s(1/2)s(1/3)\\
V^u(F_2) &= 14s(2)s(1)s(2/3) + 16s(1)s(3/2)s(5/6)s(1/3) + 6s(1)s(4/3)s(1/3)(s(1/2))^2 - (E^u(F_2))^2
\end{aligned}
$$

F_3, F_4 and F_5 have been designed so that

$$
\begin{aligned}
E^u(F_3) &= 0 \quad V^u(F_3) = 1\\
E^u(F_4) &= 0 \quad V^u(F_4) = 1\\
E^u(F_5) &= 0 \quad V^u(F_5) = 1.
\end{aligned}
$$

Before integrating F_6, we calculate

$$J(\gamma) = \int_{-1}^{1}\frac{0.5}{1+\gamma t^2}dt = \frac{1}{\sqrt{\gamma}}\text{atan}(\sqrt{\gamma}), \qquad K(\gamma) = \int_{-1}^{1}\frac{0.5}{(1+\gamma t^2)^2}dt = \frac{1}{2\sqrt{\gamma}}(\text{atan}(\sqrt{\gamma}) + \frac{\sqrt{\gamma}}{1+\gamma}). \qquad \text{Then}$$

$$
\begin{aligned}
E^u(F_6) &= 0.5J(1) + J(4)^2 + 8J(16)^3 \\
V^u(F_6) &= 0.25\ K(1) + K(4)^2 + 64\ K(16)^3 + J(1)\ J(4)^2 + 8J(1)J(16)^3 + 16\ J(4)^2J(16)^3 - E^u(F_6)^2
\end{aligned}
$$

Integrating F_7 requires the calculation of

$$
I_n(\gamma) = \frac{1}{2}\int_{-1}^{1} |t-\gamma|^n dt = \frac{1}{2(n+1)}((1-\gamma)^{n+1} + (\gamma+1)^{n+1}).
$$

We note that $I_n(-\gamma) = I_n(\gamma)$. It is then straightforward that:

$$
\begin{aligned}
E^u(F_7) &= I_3(0) + I_3(1/3)^2 + I_3(0)I_3(1/2)^2 \\
V^u(F_7) &= I_6(0) + I_6(1/3)^2 + I_6(0)I_6(1/2)^2 + \\
&+ 2\ I_3(0)I_3(1/3)^2 + 2\ I_3(0)^2I_3(1/2)^2 + 2\ I_3(1/3)^2I_3(1/2)^2I_3(0) - E^u(F_7)^2.
\end{aligned}
$$

2.5 Exact mean and variance for $\beta^{(2)}$ distribution

The mean and variance of Ishigami function for $D^{(2)}$ are

$$
\begin{aligned}
E^{(2)}(F_1) &= \frac{a}{2}(1 + \frac{45}{16\pi^4}) \\
V^{(2)}(F_1) &= (1 + \frac{45}{16\pi^4})(\frac{1}{2} + \frac{5\pi^8}{858}b^2 + \frac{\pi^4}{21}b) + \frac{a^2}{8}(3 + \frac{2835}{256\pi^4}) - E^{(2)}(F_1)^2.
\end{aligned}
$$

Considering F_2, we first calculate $\overline{s}(a)$ the counterpart of $s(a)$ for $D^{(2)}$:

$$
\overline{s}(a) = \int_{-1}^{1} \exp(at) D^2(t) dt = \int_{-1}^{1} \exp(at) D^{(2)}(t) dt = \frac{15}{16}\left(e^a(\frac{8}{a^3} - \frac{24}{a^4} + \frac{24}{a^5}) - e^{-a}(\frac{8}{a^3} + \frac{24}{a^4} + \frac{24}{a^5})\right).
$$

The mean and variance of F_2 are then expressed as:

$$
\begin{aligned}
E^{(2)}(F_2) &= 6\overline{s}(1)\overline{s}(1/2)\overline{s}(1/3) \\
V^{(2)}(F_2) &= 14\overline{s}(2)\overline{s}(1)\overline{s}(2/3) + 16\overline{s}(1)\overline{s}(3/2)\overline{s}(5/6)\overline{s}(1/3) + 6\overline{s}(1)\overline{s}(4/3)\overline{s}(1/3)(\overline{s}(1/2))^2 - (E^{(2)}(F_2))^2.
\end{aligned}
$$

The coefficients in F_3, F_4 and F_5 have been tuned to get null variance and unit mean for the uniform distribution. For the selected β distribution, these values become:

$$
\begin{aligned}
E^{(2)}(F_3) &= \frac{6\sqrt{2n}}{77} \\
V^{(2)}(F_3) &= \left((2(\frac{160}{77})^2 - \frac{1280}{77} + 8)n + (9 - 2(\frac{160}{77})^2)\right) - E^{(2)}(F_3)^2 \\
E^{(2)}(F_4) &= 0 \\
V^{(2)}(F_4) &= \left(\frac{21}{40}\right)^n \left(\frac{36}{3} - \frac{132}{5} + \frac{181}{7} - \frac{110}{9} + \frac{25}{11}\right)^n \\
E^{(2)}(F_5) &= 0 \\
V^{(2)}(F_5) &= \gamma_n^2 \left(\int_{-1}^{1} (\tanh(2u))^2 D^{(2)}(u) du\right)^n + \frac{n}{7}\eta_n^2 \ \simeq\ 0.5\left(\frac{0.6294369205482356}{2 - \tanh(2)}\right)^n + \frac{3}{14}
\end{aligned}
$$

In order to integrate F_6 we first calculate

$$\overline{J}(\gamma) = \int_{-1}^{1} \frac{D^{(2)}(t)}{1+\gamma t^2} dt = \frac{15}{16}\left(\frac{2}{3\gamma} - 2(\frac{2}{\gamma} + \frac{1}{\gamma^2}) + 2(1+\frac{1}{\gamma})^2 J(\gamma)\right), \qquad \text{and}$$

$$\overline{K}(\gamma) = \int_{-1}^{1} \frac{D^{(2)}(t)}{(1+\gamma t^2)^2} dt = \frac{15}{16}\left(\frac{2}{\gamma^2} - 2(\frac{2}{\gamma} + \frac{2}{\gamma^2})J(\gamma) + 2(1+\frac{1}{\gamma})^2 K(\gamma)\right).$$

The expressions of $E^{(2)}(F_6)$ and $E^{(2)}(F_6)$ are then easily derived

$$\begin{aligned} E^{(2)}(F_6) &= 0.5\overline{J}(1) + \overline{J}(4)^2 + 8\overline{J}(16)^3 \\ V^{(2)}(F_6) &= (0.25\ \overline{K}(1) + \overline{K}(4)^2 + 64\ \overline{K}(16)^3 + \overline{J}(1)\ \overline{J}(4)^2 + 8\overline{J}(1)\overline{J}(16)^3 + 16\ \overline{J}(4)^2\overline{J}(16)^3) - E^{(2)}(F_6)^2. \end{aligned}$$

In order to calculte the mean and variance of F_7, we introduce

$$L_{n,p}(\gamma) = \int_{-1}^{1} t^p |t-\gamma|^n dt \quad \text{and} \quad \overline{I}_n(\gamma) = \int_{-1}^{1} |t-\gamma|^n D^{(2)}(t) dt = \frac{15}{16}(L_{n,0}(\gamma) - 2L_{n,2}(\gamma) + L_{n,4}(\gamma)).$$

As $D^{(2)}(-t) = D^{(2)}(t)$, we note that $\overline{I}_n(-\gamma) = \overline{I}_n(\gamma)$. Besides, for $\gamma \in [-1,1]$, $L_{n,p}$ may be calculated splitting the domain of summation in $[-1,\gamma]$ and $[\gamma,1]$

$$L_{n,p}(\gamma) = \sum_{k=1}^{n} (-1)^{(n-k)} \begin{pmatrix} n \\ k \end{pmatrix} \left(\gamma^k \left[\frac{t^{p+n-k+1}}{p+n-k+1}\right]_{-1}^{\gamma} + \gamma^{(n-k)} \left[\frac{t^{p+k+1}}{p+k+1}\right]_{\gamma}^{1}\right).$$

The mean and variance of interest are then expressed as:

$$\begin{aligned} E^{(2)}(F_7) &= \overline{I}_3(0) + \overline{I}_3(1/3)^2 + \overline{I}_3(0)\overline{I}_3(1/2)^2 \\ V^{(2)}(F_7) &= \overline{I}_6(0) + \overline{I}_6(1/3)^2 + \overline{I}_6(0)\overline{I}_6(1/2)^2 + \\ &+ 2\ \overline{I}_3(0)\overline{I}_3(1/3)^2 + 2\ \overline{I}_3(0)^2\overline{I}_3(1/2)^2 + 2\ \overline{I}_3(1/3)^2\overline{I}_3(1/2)^2\overline{I}_3(0) - E^{(2)}(F_7)^2 \end{aligned}$$

3 INTEGRATION METHODS AND TOOLS

Various quadrature methods have been used to calculate the integrals defined in §2.

Smolyak sparse grids [30, 11, 12] have been used with Clenshaw-Curtis [5] and Gauss-Patterson [19] 1D base-quadrature. The selected computational module is Smobol by prof. Richard Dwight [7]. The two underlying 1D quadratures are associated with D^u for which they exhibit a polynomial exactness of degree $N-1$ (Clenshaw-Curtis) and $(3N-1)/2$ (Gauss-Patterson) for N points. Unfortunately, there is no 1D quadrature associated with $D^{(2)}$ available yet so that the products $F_i \times D^{(2)}$ have been integrated for the evaluation of $E^{(2)}$ and $V^{(2)}$. It is easily checked that N points then only exactly integrate a polynomial of degree $N-5$ (Clenshaw-Curtis) and $(3N-9)/2$ (Gauss-Patterson) as $D^{(2)}$ is a degree four polynomial. In the plots legend, the corresponding results are noted `SmolCC` and `SmolGP` .

All other considered methods are gPC methods [32] which basics are briefly recalled in 1D: a polynomial surrogate of F, gF, is searched for on a polynomial basis $\{P_l\}$ associated with $D(\xi)$, the probability density function of the UQ problem:

$$gF(\xi) = \sum_{l=0}^{l=M} C_l P_l(\xi) \simeq F(\xi) \qquad < P_l, P_m >= \int P_l(\xi) P_m(\xi) D(\xi) d\xi = \delta_{lm}$$

As in all other surrogate based UQ methods, the stochastic evaluations for F are estimated from gF. The mean and variance are exactly evaluated for gF as

$$E(gF) = C_0 \qquad\qquad V(gF) = \sum_{l=1}^{l=M} C_l^2$$

The coefficents of the expansion may be calculated either by quadrature using

$$C_l =< F, P_l >= \int P_l(\xi) P_l(\xi) D(\xi) d\xi,$$

or by collocation solving for the C_l the (possibly overdetermined or underdetermined) following linear system

$$\sum_{l=0}^{l=M} C_l P_l(\xi_k) = F(\xi_k) \quad \forall\ k\ \in \{1...Q\}. \tag{1}$$

The extension of this method in $\mathbb{R}^n$ is straightforward if the joint pdf of $\boldsymbol{\xi}$ is a product of 1D pdf as in our case. Finally, we remind that the polynomials orthonormal for D^u are the normalized Legendre polynomials whereas their counterparts orthonormal for $D^{(2)}$ are the normalized Jacobi polynomials with the parameters corresponding to this pdf [1].

The gPC method has been used with tensorial quadrature either for maximum degree multivariate polynomials or for total degree multivariate polynomials. The link between the retained polynomial basis and the number of quadrature points is the satisfaction of discrete orthonormality. The corresponding mentions in the plot legends are `gPC-TensGL` , `gPC-TensGJ` and `gPC-Tens-OT` (OT indicates the use of OpenTURNS[18]) – also in the legends, *m.t.* refers to maximum degree, *t.d.* refers to total degree.

Finally, two sparse gPC methods have been tested. They both search a solution to (1) with three times less collocation equations than polynomials in the total degree basis. Both also use a random sampling and the presented results correspond to the mean over four trials of the mean and variance estimations.

The first sparse gPC method is a Compressed Sensing resolution by the Basis Poursuit denoise (BPdn) algorithm [2, 3]. It solves an ϵ accurate L_1 minimization resolution of the collocation system. We have used the corresponding SPGL1 python module by E. van den Berg and M.P. Friedlander. The results of this method are referred to as `gPCBPdn` in the plot legends.

The second sparse gPC resolution is the Least Angle Regression (LAR) algorithm [4] applied to the collocation system. Its principle is to search iteratively the remaining polynomial of the basis, P_l, that is best correlated with the current expansion residual of the approximation process $r = F - \Sigma C_l^\star P_l^\star$. The corresponding results appear in plot legends as `gPC LAR OT`.

4 RESULTS

The complete set of results for the seven functions, the two pdf and the various quadrature methods is presented and discussed in reference [25]. The null mean values allow some verifications and, more important, the polynomial F_4 allows to check that the Smolyak sparse grids module and the tensorial quadratures scripts exhibit the theoretical polynomial exactness (actually, as $D^{(2)}$ is a polynomial, exactness with both D^u and $D^{(2)}$ has been checked). The next subsections focus on three specific lessons learnt.

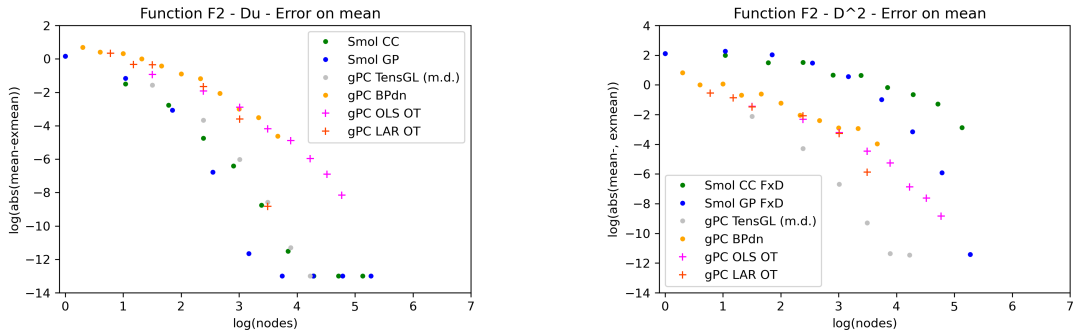

Figure 1: Convergence of $E^u(F_2)$ and $E^{(2)}(F_2)$ as function of the number of quadrature points

4.1 1D underlying quadrature in Smolyak's sparse grids

Fig. 1 presents the convergence of $E^u(F_2)$ (left) and $E^{(2)}(F_2)$ (right) as a function of the number of nodes (in logarithmic scale) for the various quadrature methods. In the left plot, it clearly appears that the theoretical properties of Smolyak sparse grids [30, 11, 12, 27] lead to the most efficient approximation of $E^u(F_2)$ by `SmolGP` and `SmolCC` among all tested numerical integration methods. Considering $E^{(2)}(F_2)$ (see **Fig. 1** right), these two sparse grids are on the contrary the least efficient methods. Most probably, the underlying 1D quadrature needs to be associated with the marginal probability law whereas, for $D^{(2)}$, due to the lack of such 1D quadrature, we have integrated $F_2 \times D^{(2)}$ by the sparse grids used for uniform distribution. Future work will include the calculation of a Gauss-Patterson 1D quadrature [19] associated with $D^{(2)}$.

4.2 Influence of coupling between input variables

We recall that functions F_2 and F_6 read

$$
\begin{aligned}
F_2(\xi) &= \exp(\xi_1 + \frac{\xi_2}{2} + \frac{\xi_3}{3}) + 2\exp(\xi_2 + \frac{\xi_3}{2} + \frac{\xi_4}{3}) + 3\exp(\xi_3 + \frac{\xi_4}{2} + \frac{\xi_5}{3}) \\
F_6(\xi) &= \frac{0.5}{1+\xi_1^2} + \frac{1}{1+4\xi_2^2}\frac{1}{1+4\xi_3^2} + \frac{2}{1+16\xi_4^2}\frac{2}{1+16\xi_5^2}\frac{2}{1+16\xi_6^2}
\end{aligned}
$$

There are hence 7 coupled pairs of input variables among 10 pairs for F_2 and only 4 coupled pairs of variables among 15 pairs for F_6. The sparsity of the exact gPC associated to F_6 (either for D^u or $D^{(2)}$) is hence superior to the one of F_2. We thus expect the sparse gPC methods `gPCBPdn` and `gPC-LAR-OT` to behave better for F_6 than for F_2. This is exactly what we observe in **Fig. 2**. Actually, these methods are the most efficient for the evaluation of $E^u(F_6)$.

4.3 Influence of random sampling in compressed sensing methods

Both sparse gPC methods, `gPC-LAR-OT` and `gPCBPdn`, use a random spampling. This raises the question of the influence of the sampling set on the accuracy of the numerical integration. It was found to be significant (up to one or one and half order of magnitude) for samplings of tenth or hundreds of evaluations and less influent for larger sampling where the change in the final

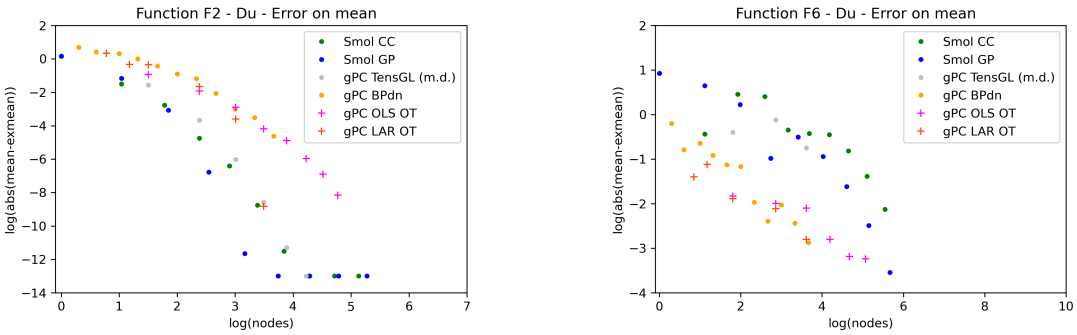

Figure 2: Convergence of $E^u(F_2)$ and $E^u(F_6)$ as function of the number of quadrature points

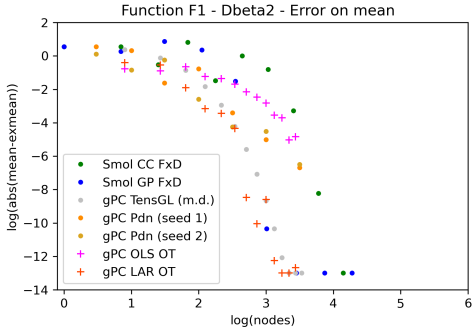

Figure 3: Convergence of $E^u(F_1)$ (F_1 Ishigami function) as function of the number of quadrature points

mean or variance accuracy was less than one order of magnitude. This is illustrated in **Fig. 3** for the `gPCBPdn` method and the Ishigami function: for each sampling size, the results obtained with two distinct samplings are reported by orange and brown circles which discrepancy can be appreciated.

5 CONCLUSION

Several numerical integration methods have been compared in intermediate dimensions for the calculation of the mean and the variance of mathematical test functions [10, 13, 25]. Most of them build a gPC [32] and the gPC exact mean and variance are the discrete evaluations of the method.

The low coupling of input variables (or, equivalently, the sparsity of the exact polynomial expansion) appeared to go with efficient evaluations of the two sparse gPC approaches [2, 3, 4]. On the contrary, the influence of the function regularity on the method accuracy is more difficult to understand based on our results. Tests should be pursued with neighboring functions exhibiting close values and distinct mathematical regularities to clarify this point.

In the future, we shall also deal with surrogates of aerodynamic functions (like lift, drag, pitching moment) from aerodynamic data basis and CFD based robust design problems. Besides ONERA has developed a strong experience in the discrete adjoint method regarding fundamental

aspects [20, 26, 28], goal-oriented simulations [22, 16, 31] and optimisation of complex configurations [6, 23, 15]. Future surrogate based numerical integration methods will hence involve adjoint-based gradient information.

6 ACKNOWLEDGEMENTS

The authors thank Sylvain Dubreuil and Nathalie Bartoli for their contribution to this work.

REFERENCES

[1] M. Abramowitz, I. Stegun. Handbook of Mathematical Functions. National Bureau of Standards. (1964)

[2] E. van den Berg, M. P. Friedlander. Probing the Pareto frontier for basis pursuit solutions". *SIAM J. on Scientific Computing*. 31(2):890-912. (2008)

[3] E. van den Berg and M. P. Friedlander. *Sparse optimization with least-squares constraints*. Tech. Rep. TR-2010-02, Dept of Computer Science, Univ of British Columbia. (2010)

[4] Blatman, G., Sudret, B. *Adaptive sparse polynomial chaos expansion based on least angle regression*. Journal of computational Physics, 230(6), 2345-2367. (2011)

[5] Clenshaw, C.W., Curtis., A.R. A method for numerical integration on an automatic computer. *Numerische Mathematik*, (2) pp 197–205 (1960)

[6] A. Dumont, A. Le Pape, J. Peter, S. Huberson. Aerodynamic shape optimization of hovering rotors using a discrete adjoint of the Reynolds-Averaged Navier-Stokes equations. *Journal of the American Helicopter Society* 56 (2011)

[7] R.P. Dwight (TU Delft) https://aerodynamics.lr.tudelft.nl/ rdwight/work_sparse.html. (2014)

[8] B. Efron, T. Hastie, I. Johnstone, and R. Tibshirani. *Least angle regression*. Annals of Statistics 32, 407499. (2004)

[9] T. Homma, A. Saltelli. Importance measures in global sensitivity analysis of nonlinear models, *Reliability Engineering & System Safety*, vol. 52 (1) ppp1–17. (1996)

[10] A. Genz. A Package for Testing Multiple Integration Subroutines, in Numerical Integration: Recent Developments, Software and Applications, edited by Patrick Keast, Graeme Fairweather, Reidel. pages 337-340. (1987)

[11] T. Gerstner, M. Griebel. Numerical integration using sparse grids. *Numerical Algorithms* 18:209. (1998)

[12] T. Gerstner and M. Griebel. Dimension-adaptive tensor-product quadrature. *Computing* Vol. 71(1):65–87. (2003)

[13] L. Kocis and W. J. Whiten. Computational investigations of low-discrepancy sequences. *ACM Trans. Math. Softw.* Vol. 23(2) pp 266–294. (1997)

[14] M. Lazareff, J. Peter, A. Fourmaux. Non-intrusive stochastic studies for external and internal flows using the *elsA* software. Proceedings of ECCOMAS CFD 2010. Lisbon. (2010)

[15] M. Meheut, A. Dumont, G. Carrier, J. Peter. Gradient-based optimization of CRM wing-alone and wing-body-tail configurations by RANS adjoint technique. AIAA Paper 2016-1293. 54th AIAA Aerospace Sciences Meeting. (2016)

[16] M. Nguyen-Dinh, J. Peter, R. Sauvage, M. Meaux, J.-A. Désidéri. Mesh quality assessment based on aerodynamic functional output total derivative. *European Journal of Mechanics B/Fluids* 45 (2014)

[17] Novak, E., Ritter, K. The Curse of Dimension and a Universal Method For Numerical Integration. Multivariate Approximation and Splines pp 177–187. (1997)

[18] Baudin, Michaël, Dutfoy, Anne, Iooss, Bertrand, Popelin, Anne-Laure. OpenTURNS: An Industrial Software for Uncertainty Quantification in Simulation, *Handbook of Uncertainty Quantification*, Springer International Publishing, 1–38. (2016)

[19] Patterson, T.N.L. The optimum addition of points to quadrature formulae Mathematics of Computation 22, 847-856. (1968)

[20] J. Peter and R.P. Dwight. Numerical sensitivity analysis for aerodynamic optimization: a survey of approaches. *Computers and Fluids* 39 (2010)

[21] J. Peter, M. Lazareff, V. Couaillier. Verification, validation and error estimation in CFD for compressible flows. International Journal of Engineering Systems Modelling and Simulation, 2(1/2):75-86 (2010)

[22] J. Peter, M. Nguyen-Dinh, P. Trontin. Goal-oriented mesh adaptation using total derivative of aerodynamic functions with respect to mesh coordinates – With application to Euler flows. *Computers and Fluids* 66 (2012)

[23] J. Peter, F. Renac, A. Dumont, M. Méheut. Discrete adjoint method for shape optimization and mesh adaptation in the *elsA* code. Status and challenges. Congrès 3AF Toulouse. (2015)

[24] J. Peter, S. Görtz, R. Graves. Three-parameter uncertainty quantification for generic missile FG5. AIAA 2017-1197. 55th AIAA Aerospace Sciences Meeting. (2017)

[25] J. Peter, S. Dubreuil, N. Bartoli. PRF MODDA Task 1.6 – Polynomial chaos for Uncertainty Quantification. RT DAAA-DTIS 1/31273. (2021)

[26] J. Peter, F. Renac, C. Labbé. Analysis of finite-volume discrete adjoint fields for two-dimensional compressible Euler flows. *Journal of Computational Physics* 449 Article 110811. (2022)

[27] J. Peter, E. Savin, I. Salah el Din. Generalized polynomial chaos and stochastic collocation method for uncertainty quantification in aerodynamics. VKI course on Uncertainty Quantification in Computational Fluid Dynamics. (2019)

[28] J. Peter, J.-A. Désidéri. Adjoint characteristics for Eulerian two-dimensional supersonic flow. arXiv:2203.12661. (2022)

[29] E. Savin, A. Resmini, J. Peter. Sparse polynomial surrogates for aerodynamic computations with random inputs. AIAA paper 2016-0433. (2016)

[30] Smolyak, S.A. Quadrature and interpolation formulas for tensor products of certain classes of functions *Dokl. Akad. Nauk SSSR* pp 240–243 (1963)

[31] G. Todarello, F. Vonck, S. Bourasseau, J. Peter, J.-A. Désidéri. Finite-volume goal-oriented mesh-adaptation using functional derivative with respect to nodal coordinates. *Journal of Computational Physics* 313 (2016)

[32] D. Xiu, G.E. Karniadakis. The Wiener-Askey polynomial chaos for stochastic differential equations. *SIAM J. Numerical Analysis* Vol. 24 pp 619-644. (2002)